



Research Paper

Degradation of the olive mill industry wastewater with sonication: Effects of some nano metal oxides on sonication

Accepted 3rd June 2019

ABSTRACT

Delia Teresa Sponza* and Rukiye Oztekin

Department of Environmental Engineering, Engineering Faculty, Dokuz Eylül University, Tinaztepe Campus, 35160, Buca/Izmir, Turkey.

*Corresponding author. E-mail: delya.sponza@deu.edu.tr. Tel: +90 232 412 11 79. Fax: +90 232 453 11 43.

The effects of nano-sized metal oxides namely titanium dioxide (TiO₂), nickel oxide (NiO) and zinc oxide (ZnO) on the ultrasound of olive mill effluent wastewater (OMW) in Izmir, Turkey were investigated. 150 min ultrasound alone provided 61, 50, 61 and 66% dissolved chemical oxygen demand (COD_{dis}), color, total phenol and total aromatic amines (TAAs) removals, respectively at 25°C. The maximum TAAs (90%), total phenol (97%), color (94%) and COD_{dis} (97%) removals were obtained with 5 mg/L nano-sized ZnO, 4 mg/L nano-sized TiO₂, 4 mg/L nano-sized TiO₂ and 4 mg/L nano-sized TiO₂, respectively throughout ultrasound.

Key words: Nano-sized titanium dioxide, nano-sized nickel oxide, nano-sized zinc oxide, olive mill effluent, ultrasound.

INTRODUCTION

Agro-industrial wastewaters such as olive-oil mill effluent wastewaters (OMW) are among the strongest industrial effluents and increasing concern has been expressed about their treatment and safe disposal, since they cause considerable environmental problems (coloring of natural waters, a serious threat to aquatic life, pollution in surface and ground waters, alterations in soil quality, phytotoxicity and odor nuisance) particularly in the Mediterranean Sea region due to its high organic chemical oxygen demand (COD), polyphenol, aromatic amines concentration, and organic content (Lafi et al., 2009). The concentration of phenolic compounds in the OMW may vary from as low as 0.05–0.2 g/L to as high as 10 g/L depending on the type and origin of the effluent (El Hajjouji et al., 2008). The TAAs in the OMW are known to be carcinogenic and toxic. Some aromatic amines containing the azo bonds (–N=N–) have complex structure and are resistant to biodegradation under aerobic conditions (El Hajjouji et al., 2008; Francioso et al., 2007).

Significant numbers of studies were focused on the efficient treatment of the OMW including various chemical, physical, physicochemical and biological treatments or

combinations of them (Lafi et al., 2009; Uğurlu and Karaoğlu, 2011). Usually, the OMW is inappropriate for direct biological treatment and the alternative treatment technologies mentioned above did not give sufficient removals for pollution parameters (COD_{dis}, total phenol, color and aromatic amines). Recently, significant interest has been shown in the application of ultrasound for the degradation of the OMW (Khoufi et al., 2004). Hydrophobic compounds with high volatility are easily and directly destroyed inside the cavitation bubbles (Pang et al., 2011). Hydrophilic organic compounds are indirectly decomposed mainly through the reaction with hydroxyl radicals (OH[•]) that is produced during cavitation process. The highly reactive OH[•] could diffuse from the cavitation bubbles to the interfacial region and bulk solution when large temperature gradient exist (Pang et al., 2011). There are three potential reaction zones in sonochemistry; that is, inside of the cavitation bubble, interfacial liquid region between cavitation bubbles and bulk liquid, and in the bulk solution (Pang et al., 2011). The collapse of cavitation bubbles near the micro-particle surface will generate high-speed microjets of liquid in the order of 100 m/s (Pang et

al., 2011). This will subsequently produce ultrasonic asymmetric shock wave upon implosion of cavitation bubbles which may cause direct erosion (damage) on the particle's surface and de-aggregation of particles to hinder agglomeration. Consequently, it will experience a decrease in particle size and an increase in reactive surface area available for the subsequent reaction. The nano-particles with the size less than that of cavitation bubbles have higher cavitation erosion resistant and are easier to approach the interfacial region (bubbles surface) during the expansion cycles of ultrasound (Pang et al., 2011). It was observed synergetic effects with the addition of various metal oxides with ultrasound to enhance the rate of degradation efficiency of organic pollutants via increasing the OH^\bullet radicals. This increases the rate of degradation of the organic compounds in wastewaters. The sonication of organic pollutants in the presence of some metal oxides (this reaction could be named as heterogeneous sonication) can easily occur in the interfacial region where very high concentration of OH^\bullet is achieved after the bubbles collapse (Pang et al., 2011). Ultrasound (US) will induce the splitting of water molecules with the presence of dissolved oxygen (Pang et al., 2011). In these reactions, ')))' denotes the ultrasonic irradiation. Thermal dissociation of water and dissolved oxygen molecules in the cavities will convert them into reactive species such as OH^\bullet , hydrogen atoms (H^\bullet), O^\bullet atoms and hydroperoxyl radicals (OOH^\bullet) in a cavitation bubble reactions (Pang et al., 2011).

Previously, the sonocatalytic degradation of some organic pollutants in aqueous solution adopting nano-sized metal oxides powder (TiO_2 , ZnO and NiO) has been reported (Pang et al., 2011). The nano-sized TiO_2 and nano-sized ZnO as photocatalyst have been widely used with ultraviolet (UV) radiation in the degradation of organic dyes due to their stability of the chemical structure, non-toxicity, optical and electrical properties. Although, these nano-sized metal oxides are non-toxic, stable and cheap, the utilization of UV increase the cost of the treatment. The nano-sized NiO nanoparticles are new class of advanced materials with very interesting features and capacity such as superior magnetic, electrical and selective adsorption properties which also has been utilized in water treatment (Pang et al., 2011). Chowdhury et al. (2010) and Zhang et al. (2012) reported that nanoporous materials such as nano-sized NiO and nano-sized TiO_2 have led to higher adsorption and catalytic efficiency with sizes varying from 17–21 nm and relatively high surface areas up to $83 \text{ m}^2/\text{g}$. Chowdhury et al. (2010) found 70% methylene blue and procion red yields using nano-sized NiO surface as adsorbent. Ahmed (2012) found 85% removal in methylene blue dye by nano-sized NiO/TiO_2 nanocomposites with photodegradation. Abu Tarboush and Husein (2012) found that the asphaltenes from a heavy oil could be adsorbed with nano-sized NiO nanoparticles with a yield of 76%. Zhang et al.

(2012) investigated the adsorption of congo red on nano-sized NiO hollow microspheres with an adsorption capacity of 526.3 mg/g , resulting in a congo red removal of 78%. However, to date, the use of nano-sized metal oxides namely, TiO_2 , ZnO and NiO in the ultrasound of the OMW for the removal of pollutants from this wastewater is yet to be studied.

In Izmir, Turkey the OMW treatment plants consisting of a combined chemical and biological process could not provide effective treatment removals. Therefore, in the present study, the effects of increasing ultrasound times (60, 120 and 150 min) and ultrasound temperature (30 and 60°C) on the removals of COD_{dis} , total phenol, color and TAAs were investigated. The main ultrasound mechanisms for the pollution parameters given above were investigated. The poly-phenols were identified and their metabolites were detected. The effects of some nano-sized metal oxides (TiO_2 , NiO and ZnO) on the removals of COD_{dis} , color, total phenol and TAAs in the OMW were investigated in a sonicator with a power of 640 W and a frequency of 35 kHz.

MATERIALS AND METHODS

Raw wastewater

The characterization of raw OMW taken from the influent of an olive oil production industry in Izmir, Turkey is shown in Table 1. This plant was operated with a three phase olive oil extraction process.

Configuration of sonicator

A Bandelin Electronic RK510 H sonicator was used for ultrasound of the OMW samples. Glass serum bottles in a glass reactor were filled to volumes of 5–500 mL with OMW and were placed in a water bath. They were then closed with teflon coated stoppers throughout the measurement of the OMW. Ultrasonic waves for 35 kHz frequency were emitted from the bottom of the reactor through a piezoelectric disc (4-cm diameter) fixed on a pyrex plate (5-cm diameter). The evaporation losses of volatile compounds were estimated to be 0.01% in the reactor and, therefore, assumed to be negligible. The serum bottles were filled with 0.10 mL methanol (CH_3OH) in order to prevent adsorption on the walls of the bottles and minimize evaporation. The temperature in the sonicator was monitored continuously and it was adjusted electronically in the sonicator with an automatic heater. The stainless steel sonicator reactor was sealed with a water jacket to maintain the desired temperature and to prevent the temperature losses. The schematic configuration of the sonicator used in this study was given elsewhere (Sponza

Table 1: Characterization of the OMW at pH=5.40 (n=3, mean values \pm standard deviation).

Parameter	Values		
	Minimum	Medium	Maximum
pH ₀	4 \pm 0.10	4.50 \pm 0.10	4.90 \pm 0.10
DO ₀ (mg/L)	0.01 \pm 0.0004	0.05 \pm 0.002	0.09 \pm 0.003
ORP (mV)	120 \pm 4.20	126 \pm 4.40	132 \pm 4.60
TSS (mg/L)	53.60 \pm 1.87	53.70 \pm 1.80	53.80 \pm 1.80
TVSS (mg/L)	34.80 \pm 1.20	35.60 \pm 1.20	36.40 \pm 1.20
COD _t (mg/L)	98780 \pm 3457	116632 \pm 4432	121560 \pm 4920
COD _{dis} (mg/L)	85400 \pm 2989	109444 \pm 3831	113500 \pm 4323
TOC (mg/L)	58510 \pm 2048	66488 \pm 2327	80450 \pm 2816
BOD ₅ (mg/L)	63800 \pm 2233	81254 \pm 2844	99130 \pm 3470
BOD ₅ / COD _{dis}	0.50 \pm 0.02	0.70 \pm 0.026	0.90 \pm 0.032
Total N (mg/L)	194 \pm 6.70	248 \pm 8.60	300 \pm 10.50
NH ₄ -N (mg/L)	23.40 \pm 0.80	30 \pm 1.05	36.60 \pm 1.20
NO ₃ -N (mg/L)	39 \pm 1.30	50 \pm 1.70	61 \pm 2.10
NO ₂ -N (mg/L)	17.60 \pm 0.60	22.60 \pm 0.70	27.50 \pm 0.90
Total P (mg/L)	492 \pm 17	630 \pm 22.05	768.60 \pm 26.90
PO ₄ -P (mg/L)	350 \pm 12.20	448 \pm 16	546.20 \pm 19.10
Total phenol (mg/L)	1332 \pm 117	2990 \pm 143	3250 \pm 180.20
Phenol metabolites			
Cathecol	2	23	26
Tyrosol	7	42	45
Quercetin	9	21	28
Caffeic acid	19	30	42
4- methyl catechol	9	15	29
2-PHE	2	4	6
3-PHE	2	9	14
TFAs (mg/L)	3050 \pm 141	3900 \pm 182	4344 \pm 222
TAAAs (mg/L)	1190 \pm 82	1990 \pm 105	2200 \pm 128
Individual TAAAs (mg/L)			
2,4,6 trimethylalanin	47	125	187
Aniline	43	83	163
o-toluidine	29	110	156
o-ansidine	45	110	129
Dimethylalanine	13	68	87
Ethylbenzene	21	110	116
Durene [1,2,4,5-tetramethylbenzene]	34	100	123
Color (m ⁻¹)	99.70 \pm 30	99.80 \pm 3.40	99.90 \pm 3.40
Oil (mg/L)	564 \pm 19	640 \pm 22.40	775 \pm 27.10

and Oztekin, 2011).

Operational conditions

Fresh solutions of nano-sized metal oxides TiO₂ (2, 4 and 8 mg/L), NiO (4, 7 and 10 mg/L) and ZnO (1, 3 and 5 mg/L)

were added to the OMW by an peristaltic pump (Watson-Marlow Bredel pumps, USA) with a flow rate of 0.10 mL/min through 5 min before ultrasound was begun at pH=5.40. Sonicated samples were taken at 60th, 120th and 150th min of ultrasound time and were kept in refrigerator with a temperature of +4°C for experimental analysis. Deionized pure water (R ¼ 18 MΩ/cm) was obtained

through a SESA Ultrapure water system.

All experiments were in batch mode by using an ultrasonic transducer (horn-type), which has five adjustable active acoustical vibration areas of 12.43, 13.84, 17.34, 26.40 and 40.69 cm², with diameters of 3.98, 4.41, 4.70, 5.80 and 7.20 cm, respectively and a maximum input power of 640 W. Five ultrasound intensities (15.70, 24.20, 36.90, 46.20 and 51.40 W/cm²) were chosen to identify the optimum intensity for maximum removal of pollutant parameters (COD_{dis}, color, total phenol and TAAs) in the OMW, while the sonicator power was 640 W. Samples were taken after 60, 120 and 150 min of ultrasound time and they were analyzed immediately as mentioned in the recent studies (Sponza and Oztekin, 2011).

Nano-sized metal oxides TiO₂, NiO and ZnO were purchased from Merck (Germany), while reagent grade perfluorohexane (C₆F₁₄) was taken from Fluka (Germany). Aniline (99%), 2-PHE (99%), 3-PHE (99%), 2, 4, 6 trimetylaniline (99%), dimethylaniline (99%) and o-toluidine (99%) were purchased from Aldrich (USA).

Analytical methods

BOD₅ and COD were monitored following Standard Methods 5210 B and 5220 D, respectively (Eaton et al., 2005). Total-N, NH₄-N, NO₃-N, NO₂-N, total-P and PO₄-P were measured with cell test spectroquant kits (Merck) in a spectroquant NOVA 60 (Merck) spectrophotometer (2003). Oil, Na⁺ and Cl⁻, total suspended solid concentration (TSS), total volatile suspended solid concentration (TVSS), dissolved oxygen (DO), pH, temperature T(°C) and oxydation reduction potential (ORP, mV) were determined following Standard Methods 5520 B, 3550, 2540 C, 2540 E, 2550, 2580, respectively (Eaton et al., 2005). The measurement of color was carried out following the methods described by Olthof and Eckenfelder (1976). To identify the TAAs, OMW (25 mL) was acidified at pH=2 with a few drops of 6 N HCl and extracted three times with 25 mL of ethyl acetate. The pooled organic phases were dehydrated on sodium sulphate, filtered and dried under vacuum. The residue was silylated with bis(trimethylsilyl)trifluoroacetamide (BSTFA) in dimethylformamide and analyzed by gas chromatograph-mass spectrometer (GC-MS). Mass spectra were recorded using a VGTS 250 spectrometer equipped with a capillary SE 52 column (0.25 mm ID, 25 m) at 220°C with an isothermal program for 10 min. TAAs were measured using retention times and mass spectra analysis. The total phenol was monitored as follows: 40 mL of OMW was acidified to pH=2 by the addition of concentrated HCl. Phenols were then extracted with ethyl acetate. The organic phase was concentrated at 40°C to about 1 mL and silylized by the addition of N,O-bis(trimethylsilyl)acetamide (BSA). The

resulting trimethylsilyl derivatives were analysed by GC-MS (Hewlett-Packard 6980/HP5973MSD). 2-PHE and 3-PHE concentrations were determined with Shimadzu CLASS-VPV6.14SP2 with Phenomenex Hyperclone 125 mm x 4.6 mm x 5 µm HPLC column using an ultraviolet (UV) method (Silva et al., 2007). Aniline, 2,4,6 trimetylaniline and dimethylaniline measurements were carried out using a high pressure liquid chromatograph (HPLC) (Agilent-1100) with a C-18 reverse phase HPLC column (25 cm x 4.6 mm, 5 µm (Ace 5C-18)) following the method developed by EPA (Bertin et al., 2001). Detection was performed at 280, 214 and 216 nm wavelengths using a UV detector for aniline, 2,4,6 trimetylaniline and dimethylaniline, respectively. o-toluidine was determined using a HPLC (Agilent-1100) with a Spectra system model SN4000 pump and Asahipak ODP-506D column (150 mm x 6 mm x 5 µm). o-anisidine was measured in a HPLC (Agilent -1100) with UV detector at a mobile phase of 35% acetonitrile/65% H₂O at a flow rate of 1.2 mL min⁻¹. The column was 50 cm x 2 mm ID stainless steel packed with µ-Bondapak C-18. Ethylbenzene and durene (1,2,4,5-tetramethylbenzene) measurements were performed with a GC-MS (GC-MS Agilent Technologies, 7890A (G3440A) GC System, 5975C Inert MSD7683B Series Injector) containing inlet split/splitless ratio of 50:1 with a HP-1 polymethylsiloxane 30 m x 0.32 mm x ID 0.25 µm film thickness column (Hewlett-Packard) at 240°C. The carrier was helium (He) with a flowrate of 1.4 mL min⁻¹ and column 60 m x 0.25 mm x ID 0.25 µm. The steady-state OH ion concentration [OH[•]] throughout sonication was calculated following the method proposed by Villeneuve et al. (2009) while the second-order reaction kinetics of aromatic amines and phenols were determined by Bertin et al. (2001) and Silva et al. (2007).

All experiments were carried out three times and the results are given as the means of triplicate samplings. The data relevant to the individual pollutant parameters in OMW (COD, color, phenol and TAAs) are given as the mean with standard deviation (SD) values.

RESULTS AND DISCUSSION

Role of ultrasound frequency, ultrasound power, ultrasound intensity and power density on the removals of COD_{dis}, color, total phenol and TAAs removals in OMW

Five different ultrasound frequencies (25, 35, 132, 170 and 350 kHz) was researched under ambient conditions (25°C), at constant ultrasound power (640 W) to determine the optimum ultrasound frequency for maximum COD_{dis} removals in the OMW (Table 2). Among the frequencies used in the ultrasound process (25, 35, 132, 170 and 350 kHz), it was found that an ultrasound frequency of 35 kHz is

Table 2: Sonicational parameters and corresponding values of sonication process in this study at pH=5.40 after 150 min ultrasound time for maximum COD_{dis} yields under ambient conditions (at 25°C).

Ultrasound parameter	The corresponding values of sonication process				
Ultrasound frequency (kHz)	25	35	132	170	350
Ultrasound power (W)	120	640	350	3000	5000
Power density (W/mL)	0.10	2.14	0.90	1.65	1.90
Ultrasound intensity (W/cm ²)	15.70	51.40	24.20	36.90	46.20
Specific energy (kWh/kg COD _{influent})	2.40	11.50	3.10	4.10	5.10
COD removal efficiency (%)	45	61	47	53	58

Table 3: Effect of increasing ultrasound time (60, 120 and 150 min) and increasing temperature (at 25°C, at 30°C and at 60°C) on the COD_{dis}, total phenol, color and TAAs removal efficiencies in OMW, at an initial COD_{dis} concentration=109444 mg/L, at an initial total phenol concentration=2990 mg/L, at an initial color concentration=99.80 m⁻¹, at an initial TAAs concentration=1990 mg benzidine/L, at ultrasound power=640 W, at ultrasound frequency=35 kHz and at pH=5.40 (n=3, mean values).

SET	Parameter	Removal Efficiencies (%) ^a								
		25°C (Control) ^b			30°C			60°C		
		60. min ^c	120. min ^c	150. min ^c	60. min ^c	120. min ^c	150. min ^c	60. min ^c	120. min ^c	150. min ^c
1	COD _{dis} ^d	13 ^a	42 ^a	61 ^a	16 ^a	42 ^a	63 ^a	18 ^a	47 ^a	67 ^a
2	Total phenol ^d	30 ^a	57 ^a	61 ^a	45 ^a	62 ^a	80 ^a	48 ^a	70 ^a	88 ^a
3	Color ^e	36 ^a	48 ^a	50 ^a	39 ^a	53 ^a	75 ^a	45 ^a	70 ^a	84 ^a
4	TAAs ^f	41 ^a	52 ^a	66 ^a	47 ^a	56 ^a	69 ^a	62 ^a	71 ^a	79 ^a

^a Removal efficiency (%); ^b 25°C (Control): without the addition of nano-sized metal oxides (TiO₂, ZnO and NiO) at 25°C in OMW at pH=5.40; ^c min: increasing ultrasound time (60th, 120th and 150th minute); ^d initial concentrations of COD_{dis} and total phenols (mg/L); ^e initial concentrations of color (m⁻¹); ^f initial concentrations of TAAs (mg benzidine/L).

the optimum frequency for maximum COD_{dis} removal (61%) in the OMW after 150 min ultrasound at 25°C (Table 2). Increasing the ultrasound frequencies > 35 kHz did not increase the number of OH[•] radicals (David, 2009). A more energetic implosion of cavitation bubbles is expected to occur at low frequency rather than at high frequency because of a larger bubbles radius observed at low frequency (David, 2009). The size of bubbles formed in H₂O, is inversely proportional to the frequency of the wave. 120, 350, 640 and 3000 W ultrasound powers was researched under ambient conditions (at 25°C), at constant ultrasound frequency (35 kHz) to determine the optimum ultrasound power for maximum COD_{dis} removals in the OMW (Table 2). Among the powers used, it was found that a ultrasound power of 640 W is the optimum power for maximum COD_{dis} removals (61%) in the OMW after 150 min ultrasound at 25°C (Table 2). In general, when ultrasonic irradiation is used, the degradation ratio gradually becomes higher when the output power of the ultrasound is increased from 120 to 640 W. The sono-degradation of pollutants increased with increasing applied power. As the power increased, the number of collapsing cavities also increased, thus leading to enhanced degradation rates, thus resulting in high OH[•] production and COD_{dis} removal. Because the formation of cavitation bubbles and the extent of bubble collapse

depends on the sound intensity, various ultrasound intensities were compared for their impacts on the COD_{dis} removals. In this study, the optimum cavitation threshold was 51.40 W/cm² for the maximum removals of COD_{dis} (61%) at 25°C after 150 min ultrasound time (Table 2). For the maximum COD_{dis} removal, the specific energy was 11.50 kWh/kg COD_{dis} in the influent (Table 2).

Effect of increasing ultrasound time and temperature on the COD_{dis}, total phenol, color and TAAs removal efficiencies in the OMW

The OMW samples were sonicated at 30 and 60°C during 60, 120 and 150 min ultrasound times (Table 3). Increasing the ultrasound time from 60 to 120 min enhanced the COD_{dis} removals under ambient conditions (at 25°C). The maximum COD_{dis} removal was 61% after 150 min ultrasound time, at 25°C and at pH=5.40 (Table 3). 16, 42 and 63% COD_{dis} removals were measured after 60, 120 and 150 min ultrasound time, respectively at pH=5.40 and at 30°C (Table 3). The maximum COD_{dis} removal was 67% after 150 min ultrasound time, at pH=5.40 and at 60°C (Table 3). An initial increase in solution temperature increases the rate of reaction, leading to a greater fraction

of OH ion production and volatile compounds partitioning into the cavity. A further increase in solution temperature leads to a decrease in the rate of reaction (Sponza and Oztekin, 2011). The treatment by ultrasound converts COD_{dis} in the OMW to much smaller sonodegraded compounds. Short ultrasound times (60 min) did not provide high degradation removals for refractory COD throughout ultrasonic irradiation. COD_{dis} was not completely removed under the ultrasonic action even with a long ultrasound time (150 min) in OMW. This was probably caused by insufficient levels of OH[•] formation. Hence, COD_{dis} do not have the ability to attack at low concentrations of OH[•], thus leading to decreased sonodegradation rates of COD_{dis} as reported by David (2009).

The COD_{dis} removals obtained in the OMW were higher than those of the recent studies obtained at 25°C with ultrasound. In a study performed by Atanassova et al. (2005), a COD_{dis} removal of 45% was found after 240 min ultrasound time at a power of 150 W and a frequency of 80 kHz at 25°C. Benedito et al. (2004) observed a 40% COD_{dis} removal in the OMW containing 10 mg/L alpechin at 40 kHz frequency, at 700 W power, after 15 min ultrasound time, at 50°C. Canizares-Macias et al. (2004) found 56% COD_{dis} removal at 25°C temperature, 20 kHz frequency, and at a power of 400 W, after 60 min ultrasound time by an ultrasound system assisted with Rancimat Method. In this study, the maximum COD_{dis} removal (61%) at 25°C is higher than the data obtained by Atanassova et al. (2005) at 25°C, by Benedito et al. (2004) at 50°C and by Canizares-Macias et al. (2004) at 25°C. This could be attributed to the different increasing temperature, the different ultrasound frequency, the different ultrasound power and the different ultrasound time used throughout sonication.

In this study, it was found that the total phenol removal efficiencies in the OMW increased from 30% up to 57% as the ultrasound time was increased from 60 to 120 min at 25°C and pH=5.40. The maximum total phenol removal efficiency was 61% after 150 min ultrasound time, at pH=5.40 and at 25°C (Table 3, SET 2). 48, 70 and 88% total phenol removals were found after 60, 120 and 150 min ultrasound time, respectively at pH=5.40 and at 60°C (Table 3, SET 2). The maximum total phenol removal was 88% after 150 min ultrasound time, at pH=5.40 and at 60°C (Table 3, SET 2). The Kruskal-Wallis test statistics showed that the effects of increasing ultrasound time (from 60 up to 120 and 150 min) and temperature (from 25°C to 30 and 60°C) on the total phenol removals did not differ and as such, not significant (Mann-Whitney *U*-test statistic=2.98, $p < 0.10$) after 60 and 120 min at all increasing temperatures. Although, the increase in ultrasound times increase the total phenol removals, the temperature increase from 25 up to 60°C did not contribute to total phenol removals after 60 and 120 min ultrasound time. However,

the increase in temperature contributed to the total phenol removals after 150 min ultrasound time. The total phenol removals significantly differed (Mann-Whitney *U*-test statistic=11.02, $p < 0.1$).

The degradation of phenol occurs in the bulk liquid medium due to hydroxylation reaction induced by OH[•] generated from cavitation bubble. This is a consequence of low vapor pressure of phenol (due to which it does not evaporate into the cavitation bubble) and the hydrophilic nature of the phenol molecule. Higher ultrasound times are needed for complete mineralization of phenol. Short ultrasound times (60 min) did not provide high degradation removals for refractory part of phenolic organics throughout ultrasonic irradiation since the OH[•] radicals can not have enough time to binding to the phenol. Phenol was not completely removed under the ultrasonic action even with a long ultrasound time (150 min) in the OMW.

Around 36, 48 and 50% color removals were obtained at 60 and 150 min ultrasound time, respectively, at an initial color level of 99.80 m⁻¹ in the OMW under ambient conditions (at 25°C) (Table 3). 39, 53 and 75% color removals were found after 60, 120 and 150 min ultrasound time, respectively at pH=5.40 and at 30°C. 45, 70 and 84% color removals were observed after 60, 120 and 150 min ultrasound time, respectively, at pH=5.40 and at 60°C (Table 3). The maximum color removal was 84% after 150 min ultrasound time, at pH=5.40 and at 60°C.

Although, the color yields increased as the ultrasound time was increased from 60 to 120 min, the contribution of low temperature on the color yields was found not to be significant. Kruskal-Wallis test statistics showed that the color removals did not differ significantly after 60 and 120 min ultrasound times, at 30°C (Mann-Whitney *U*-test statistic=2.38, $p=0.05$) Low color removals in the OMW effluents showed that low ultrasound temperature (25°C) is not able to achieve the complete removal of the colored organics (e.g. lignin, organic acids, etc.) and the phenolic compounds (e.g. tannins, antocyanins, catechins, etc.). This might be due to the generation of high concentration of intermediate compounds that cannot be further oxidized by OH[•] and consequently are accumulated in the system. It was found that high temperature such as 60°C increased significantly the color yields after 150 min ultrasound time. The Kruskal-Wallis test statistics showed that the color removals differed after 150 min ultrasound time at a temperature of 60°C and these differences are significant (Mann-Whitney *U*-test statistic=12.63, $p=0.05$). The increasing temperature is likely to facilitate the bubble formation due to an increase of vapour pressure of a medium and so lead to easier cavitation with less violent collapse.

41, 52 and 66% TAAs removal efficiencies were observed at an influent TAAs concentration of 1990 mg/L after 60, 120 and 150 min ultrasound time, respectively, at pH=5.40

Table 4: H₂O₂ and OH[•] ion concentrations in the OMW at 60°C, after 30, 120 and 150 min ultrasound time, at an initial COD_{dis} concentration=109444 mg/L, at an initial color concentration=99.80 m⁻¹ and at an initial TAAs concentration=1990 mg/L, respectively, at pH=5.40 at ultrasound power=640 W and at ultrasound frequency=35 kHz (n=3, mean values).

Conditions	COD _{dis} removal		Color removal		Aromatic amines removal		Phenol removal	
	H ₂ O ₂ ^a	OH [•] ^a	H ₂ O ₂ ^a	OH [•] ^a	H ₂ O ₂ ^a	OH [•] ^a	H ₂ O ₂ ^a	OH [•] ^a
H ₂ O ₂ concentration (mg/L) in deionized water (60°C) at pH=7.0 at the beginning	177	0	177	0	0	0	209	0
H ₂ O ₂ concentration (mg/L) in deionized water (60°C) at pH=7.0 after 150 min ultrasound time	176	0	176	0	0	0	198	0
H ₂ O ₂ concentration (mg/L) in OMW (60°C) at pH=5.40 at the beginning	34	1 * 10 ⁻⁹²	49	1 * 10 ⁻⁸²	175	1 * 10 ⁻²⁷²	98	25 * 10 ⁻⁸²
H ₂ O ₂ concentration (mg/L) in OMW (60°C) after 30 min ultrasound time at pH=5.40	156	10 * 10 ⁻⁶²	160	1 * 10 ⁻⁵²	174	1 * 10 ⁻²⁶²	185	10 * 10 ⁻⁶²
H ₂ O ₂ concentration (mg/L) in OMW (60°C) after 120 min ultrasound time at pH=5.40	92	13 * 10 ⁻¹⁵	73	9 * 10 ⁻¹²	174	1 * 10 ⁻²⁵²	145	2 * 10 ⁻⁵²
H ₂ O ₂ concentration (mg/L) in OMW (60°C) after 150 min ultrasound time at pH=5.40	11	16 * 10 ⁻⁷	5	9 * 10 ⁻⁵	173	1 * 10 ⁻²⁴²	14	43 * 10 ⁻⁷

^a Concentration (mg/L).

and at 25°C (Table 3). As the temperature increased to 30°C, the TAAs removals increased to 47, 56 and 69% after 60, 120 and 150 min ultrasound time, respectively at pH=5.40 (Table 3). 62, 71 and 79% TAAs removal efficiencies were found after 60, 120 and 150 min ultrasound time, respectively at pH=5.40 and at 60°C (Table 3). The maximum TAAs removal efficiency was 79% after 150 min ultrasound time, respectively at pH=5.40 and at 60°C (Table 3).

Although, the increasing ultrasound time contribute to the TAAs removals, the Kruskal–Wallis test statistics showed that the TAAs removals did not differ significantly after 60 min ultrasound time, at 30 and at 60°C (Mann–Whitney *U*-test statistic=1.09, *p*=0.05). The increasing of temperature and ultrasound time from 25 to 30 and to 60°C and from 120 to 150 min ultrasound time, respectively, increased the TAAs removals. The Kruskal–Wallis test statistics showed that the TAAs removals differed after 150 min ultrasound time versus increasing temperature and

these differences were significant (Mann–Whitney *U*-test statistic=13.88, *p*=0.05).

Removal mechanisms of COD_{dis}, total phenol, color and TAAs in the OMW throughout ultrasound

The H₂O₂ measurements were performed in the absence and in the presence of OMW throughout ultrasound of TAAs, color, total phenol and COD_{dis} at 30°C after 150 min ultrasound time, in order to detect the ultrasound mechanisms of the parameters in suspension. In the absence of OMW (in deionized water) the H₂O₂ was accumulated (176 mg/L). Similarly, the H₂O₂ concentration remained as formed after 150 min ultrasound time (Table 4). The initial rate of H₂O₂ formation associated with the COD_{dis} treatment by ultrasound in the OMW decreased significantly with increasing ultrasound time at 60°C (Table 4). The H₂O₂ concentration was 34 mg/L at the beginning of

the ultrasound in the OMW and then increased to 156 mg/L with the production of OH^\bullet ion since H_2O_2 is formed by the recombination of OH^\bullet throughout sonolysis. Afterwards, the H_2O_2 concentrations decreased to 92 and 11 mg/L with the OH^\bullet ion increase. The OH^\bullet ion concentrations increased from $10 \cdot 10^{-62}$ to $16 \cdot 10^{-7}$ mg/L after 150 min ultrasound time in the OMW. This showed that hydroxylation is the main mechanism for the removal of COD_{dis} .

In the absence of the OMW (in deionized water), the H_2O_2 concentration was measured as 209 mg/L at pH=7.0, while the H_2O_2 concentration decreased slightly and remained around 198 mg/L after 150 min ultrasound time, at pH=5.40 throughout ultrasound of phenols (Table 4). The H_2O_2 concentration was 98 mg/L at the beginning of the ultrasound in the OMW and then increased to 185 mg/L after 30 min ultrasound time with the production of OH^\bullet ion since H_2O_2 is formed by the recombination of OH^\bullet throughout sonolysis. Afterwards, the H_2O_2 concentrations decreased to 145 and 14 mg/L with the OH^\bullet ion increase in the OMW after 120 and 150 min ultrasound time, respectively. The H_2O_2 values in the OMW are much lower when compared with those in deionized water (at a neutral pH=7.0) due to the fact that in the former case, many of the OH^\bullet produced by ultrasound reacted with phenol before they could combine to form H_2O_2 . The OH^\bullet ion concentrations reached $25 \cdot 10^{-82}$ mg/L from $43 \cdot 10^{-7}$ mg/L after 150 min ultrasound time in the OMW. This showed that hydroxylation is the main mechanism for the removal of phenol. In this study, in the OMW, the most sonogenerated OH^\bullet reacted with 93% maximum total phenol removal and radical recombination to produce H_2O_2 after 150 min ultrasound time. Different phenol removal mechanisms and metabolites were reported throughout ultrasound. Pétrier et al. (1994) investigated the sonolysis of phenol in aqueous solution and found hydroquinone, catechol, and benzoquinone as reaction products. These reaction products are attributed to the attack of the OH^\bullet on phenol. Similarly, Anju et al. (2012) showed that the OH^\bullet was involved in the degradation pathways of phenol. They reported that OH^\bullet was generated from the dissociation of H_2O during ultrasonic irradiation process, and very high concentration of OH^\bullet is achieved after the bubbles collapse. The concentration that could be reached is estimated to be as high as 4 mM. However, Currell et al. (1963) found that the ultrasound of phenol was sono-degraded partially by pyrolysis in the bubble phase. This could be due to the reactor configuration and geometry, the wastewater characteristics ultrasound intensity, frequency and the presence of matrix components in the wastewater researched.

Throughout ultrasound of the colored organics and phenols in the OMW, the H_2O_2 production decreased while the OH^\bullet ion concentration increased. Since the sonooxidation of the COD_{dis} and the colored organic substances comprised 63 and 75% of the total

sonodegradation process at 30°C after 150 min ultrasound time, OH^\bullet is the major process for complete degradation of these parameters. Throughout the sonodegradation of the TAAs the rate of OH^\bullet production was zero. This accomplished with H_2O_2 concentration as low as $1 \cdot 10^{-272}$ mg/L (Table 4). Therefore, it can be seen that OH^\bullet is not the major process for complete degradation of the aromatic amines. In other words, in this study, the contribution of OH^\bullet was minor for the ultimate sonodegradation of aromatic amines. The formation of by-products (aniline, o-toluidine, anisidine, dimethylaniline and dimethylaniline) for possible OH^\bullet oxidation was not observed in HPLC. Similar results were obtained in the studies performed by Wu and Ondruschka (2005). The contribution of the pyrolysis to the destruction of TAAs is significant. The occupation of the heart and/or the surrounding shell of the bubble by TAA molecules limit the sonolysis of H_2O and the formation of OH^\bullet . This indicates that the main process for the destruction of TAAs is pyrolysis. The addition of 600 mg/L 1-butanol to the OMW very slightly affected (4%) the TAAs removals by the OH^\bullet scavenger (data not shown) while about 67-59% inhibition was observed for COD_{dis} and color removal (data not shown). Throughout ultrasound of TAAs, some gaseous by-products were observed in the headspace of the ultrasound reactor. 31.20 - 41.11% CO_2 and 16 - 18.32% NH_3 were measured after 10 min ultrasound time in the headspace of the sonicator reactor (data not shown). It can be assumed that these gases are primarily formed as soon as TAAs penetrate the cavitation bubbles in order to be pyrolyzed. The oxidation of TAAs with OH^\bullet appears to be of relatively minor importance, because of the low inhibition of the sono-degradation by means of 1-butanol and since the expected steady-state OH^\bullet concentration in the interfacial region of the cavitation bubble, where TAAs accumulate, is lower and not sufficient for a complete degradation of TAAs. The TAAs are then expected to be mainly localized in the heart and/or in the surrounding shell of the bubble, inhibiting the production of OH^\bullet and hence the oxidation pathway.

In this study, the ultrasound mechanism of the AAs in the OMW are attributable to the priority of cleavage of azo links by pyrolysis. Throughout pyrolysis, OH^\bullet initially diffuse into their long-lived cavity bubbles to undergo pyrolytic destruction inside the collapsing bubble and then the cleavage of azo groups open the $\text{N}=\text{N}$ bonds. The cleavage of methyl, ethyl and C-H-O bonds can destroyed the aromatic structures in TAAs namely, o-toluidine, dimethylaniline, ethylbenzene and durene.

Effects of nano-sized metal oxides (TiO_2 , NiO and ZnO) on the sonodegradation of COD_{dis} , total phenol, color and TAAs in the OMW

Keeping the conditions of 35 kHz, 640 W and 21°C,

Table 5: Effects of some nano-sized metal oxides (TiO₂, NiO and ZnO), on the removal of COD_{dis}, total phenol, TAAs and color at 25°C, after 150 min ultrasound time, at a frequency of 35 kHz, at a power of 640 W and at pH=5.40 (n=3, mean values).

Nano-sized metal oxides and their concentrations	Sonodegradation removals (%) ^a			
	COD _{dis} ^a	Phenol ^a	TAAs ^a	Color ^a
Control (without nano-sized metal oxides)	61	61	66	50
nano-sized TiO ₂ = 2 mg/L	92	90	86	85
nano-sized TiO ₂ = 4 mg/L	97	97	88	94
nano-sized TiO ₂ = 8 mg/L	90	94	83	90
nano-sized NiO = 4 mg/L	66	84	84	83
nano-sized NiO = 7 mg/L	89	91	88	88
nano-sized NiO = 10 mg/L	85	88	85	90
nano-sized ZnO = 1 mg/L	64	86	74	80
nano-sized ZnO = 3 mg/L	72	90	89	88
nano-sized ZnO = 5 mg/L	92	93	90	93

^a Sonodegradation removals (%).

ultrasonic degradation of COD_{dis}, TAAs, total phenol and color in the OMW were investigated in the presence of nano-sized metal oxides TiO₂, NiO and ZnO. Table 5 shows the effect of nano-sized metal oxides on the removal of the pollutant parameters given above in the OMW samples. The contribution of nano-sized TiO₂ on COD_{dis}, TAAs, total phenol and color yields was found to be significant. Although, 2 mg/L nano-sized TiO₂ increased significantly the COD_{dis} (92%), TAAs (86%), total phenol (90%) and color (85%) (Table 5). The maximum COD_{dis} (97%), TAAs (88%), total phenol (97%) and color (94%) yields were obtained at 4 mg/L nano-sized TiO₂ concentration. The increasing nano-sized TiO₂ to 8 mg/L decreased the removals in the aforementioned pollution parameters. Nano-sized TiO₂ particles provides more chances for the organic compounds (COD_{dis}) phenol and TAAs) to adsorb on the surface of the nano-sized TiO₂ particles to be directly composed by holes. Throughout ultrasound of the OWW with semiconductor nano-sized TiO₂, firstly, the formation of the light at wavelength below 375 nm occurred. Under these conditions, the light can excite the semiconductor nano-sized TiO₂ acting as a photocatalyst, and OH[•] radicals with oxidative performance activate the surface of the nano-sized TiO₂. Secondly, the temperature of hot spot produced by ultrasonic cavitation in the sonicator can achieve high temperatures such as 102 and 104°C. As a result, temperatures as high as 104°C bring many holes producing OH[•] radicals on the surface of the nano-sized TiO₂. Throughout ultrasound, the steps of treatment of the OMW include the following steps: (i) the mass transfer of the pollutants (COD_{dis}, phenol, TAAs and color giving organics) from the bulk solution to the surface of nano-

sized TiO₂, (ii) adsorption of pollutants onto the nano-sized TiO₂ surface (iii) chemical reactions (OH[•] and other radical productions) on the surface of nano-sized TiO₂. Desorption of the products is from the nano-sized TiO₂ surface during oscillation and mass transfer of the product is from the nano-sized TiO₂ surface to the bulk solution of the OMW in the sonicator (Khoufi et al., 2004). At low nano-sized TiO₂ concentrations the adsorbed pollutant molecules on nano-sized TiO₂ surfaces decrease in the OMW. Therefore, the degradation ratio of the pollutants decreased since the organics did not find enough holes in the surface of the nano-sized TiO₂ nano-particles. Thus it reduces the formation rate and number of OH[•] radicals and inhibits the generation of OH[•]. At high nano-sized TiO₂ concentrations the COD_{dis}, total phenol, TAAs and color removals decreased. This could be attributed to the aggregation of nano-sized TiO₂ particles at high concentrations, causing a decrease in the number of active surface sites, and decrease in the passage of sonic waves through sonication of the OMW samples. Wang et al. (2008) also reported that high nano-sized TiO₂ concentrations (≥ 6-12 mg/L) decrease the COD_{dis} removals. The increase in sono-destruction of pollutants at 4 mg/L nano-sized TiO₂ may be explained by the cavitation process which produces higher surface area. The ultrasonic waves do not only destroy the phenol compounds through cavitation process but also could increase the adsorption process by increasing the surface area of the nano-sized TiO₂ catalyst as reported by Laxmi et al. (2010). During the ultrasound of the OMW with nano-sized TiO₂, more active free radicals, such as OH[•] and O₂H[•] were produced from the dissociation of the H₂O and H₂O₂ (Laxmi et al., 2010). In this study, the maximum TAAs

removal (88%) observed in 4 mg/L nano-sized TiO₂ at 30°C was higher than the removal obtained by Cardoso et al. (2010) for 4,4-oxydianiline aromatic amines removal (81%) with 5 mg/L nano-sized TiO₂ after 150 min ultrasound. In a study performed by Khochawala and Gogate (2010), it was observed that 2 g/L nano-sized TiO₂ is the optimum concentration for maximum phenol (78%) removal. The removals obtained in our study are comparably higher than that the literatures mentioned above. Among the nano-sized ZnO doses used in this study, the maximum COD_{dis} (92%), TAAs (90%), total phenol (93%) and color (93%) were obtained at a nano-sized ZnO concentration of 5 mg/L (**Table 5**). At low nano-sized ZnO doses, the removal efficiencies of the pollution parameters given above decreased. Nano-sized ZnO particles have been used to bind to the pollution parameters in wastewaters throughout ultrasound due to their surface properties, porosity, size distribution, density and surface charges. Throughout ultrasound of the OMW in the presence of nano-sized ZnO particles, ultrasound acted as a deaggregator by microstreaming and causing microbubble collapse, which induced surface cleaning of the nano-sized ZnO particles: (i) US acted as a deaggregator by microstreaming and causing microbubble collapse, which induced surface cleaning of the ZnO particles; (ii) the presence of an additional liquid–solid interface in the liquid bulk promotes cavitation, and (iii) ultrasound (US)-accelerated mass transfer occurs between the solution phase and the nano-sized ZnO surface (Anju et al., 2012; Wu, 2008). The nano-sized ZnO nanoparticles help to break up the microbubbles created by ultrasound into smaller ones, thus increasing the number of regions of high temperature and pressure (Wu, 2008). This leads to increase in the number of OH• radicals which will interact with the organic molecules present in H₂O and oxidise them, resulting in eventual mineralization. In the increase in degradation removals of COD_{dis}, phenol rate can be attributed to the increase in the number of active cavitation bubbles and consequent generation of more OH• radicals. At high nano-sized ZnO concentration (>10 mg/L), the aggregation of nano-sized ZnO nanoparticles causes decrease in surface holes (Wang et al, 2008). This leads to decrease in the formation of OH• radicals, resulting in low sonolytic efficiency. Beyond the optimum nano-sized ZnO concentration (3 mg/L), the degradation slows down and thereafter remains more or less steady or even decreases. The enhanced degradation efficiency is probably due to increased number of OH• radicals and their interactions. Another reason may be the aggregation of nano-sized ZnO particles causing decrease in the number of available nano-sized ZnO surface sites for binding of OH• radicals. The particles cannot be fully and effectively suspended beyond a particular loading in the sonicator. Anju et al. (2012) found 63, 62 and 73% phenol yields in the presence of 10 mg/L nano-sized ZnO under US, UV and combination of UV

and US irradiation conditions after 2 h of exposure time. In another study by Drijvers et al. (1999), the decomposition of phenol and COD_{dis} were investigated using nano-sized metal oxides Al₂O₃, ZnO and NiO under the combined effect of sonolysis at 520 kHz and chemical oxidation with H₂O₂. Thus, 67, 68 and 70% phenol yields were obtained with the metal oxides mentioned above. These COD_{dis} and phenol yields in these studies were lower than the data of the present study. This could be attributed to the differences in wastewater, nano-sized ZnO concentrations and sonication operational conditions. pH affects the nano-sized ZnO surface properties, phenol, TAAs dissociation and OH• formation (Wang et al., 2008). Hydroxyl anions (OH⁻) in alkaline solution typically act as scavenger of holes on the surface of nano-sized ZnO particles and become OH• with strong oxidation ability after they lose one electron. Consequently, the probability of generating OH• increases with pH (Wang et al., 2008). Nano-sized ZnO is known to be an effective oxidation catalyst as it could promote the formation of reactive radicals to oxidize organic compounds to lower carbon organic compounds even to CO₂ and H₂O (Anju et al., 2012).

In this study, the maximum COD_{dis} (89%), TAAs (88%), total phenol (91%) and color (88%) yields were obtained at a nano-sized NiO concentration of 7 mg/L (**Table 5**). At low (4 mg/L) and high (10 mg/L) nano-sized NiO doses, the removal efficiencies of the pollution parameters given above decreased (**Table 5**). Dissociation of water in the cavitation bubbles throughout ultrasound will convert it into reactive species such as OH•, H• and OOH• (Sponza and Oztekin, 2011). H₂O₂ will be formed outside the hot bubbles or at the cooler interface as a consequence of OH• and OOH• recombination. On the other hand, the H• and OH• species may further react with H₂O₂. The presence of 7 mg/L nano-sized NiO increase the number of free radicals generated, thereby increasing the rate of degradation of the COD_{dis}, phenol and TAAs in the OMW. The nano-sized NiO nanoparticles with the size less than that of cavitation bubbles have higher cavitation erosion resistant and are easier to approach the interfacial region (bubbles surface) during the expansion cycles of ultrasound (Srivastava et al., 2003). Throughout ultrasound for the removals of pollutants from the OMW contained: mass transfer of the pollutants from the bulk solution to the surface of nano-sized NiO, adsorption of pollutants onto the nano-sized NiO surface during oscillation, chemical reactions (OH• and other radical productions) on the surface of nano-sized NiO, Desorption of the products from the nano-sized NiO surface during oscillation and mass transfer of the product from the nano-sized NiO surface to the bulk solution steps. A nano-sized NiO system was used as a catalyst for low-temperature oxidation of phenol (Srivastava et al., 2003). Nano-sized NiO is also being used as a catalyst for the oxidation of CO (Srivastava et al., 2003). The catalytic properties of nano-sized NiO depend on the number of

Table 6: Measurements of phenol metabolites (catechol, 4-methyl catechol, tyrosol, quercetin, caffeic acid, 2-PHE and 3-PHE) in the OMW with the addition of some nano-sized TiO₂, NiO and ZnO oxides with HPLC after 150 min ultrasound time at pH=5.40, at an initial total phenol concentration=2990 mg/L, at ultrasound power=640 W, at ultrasound frequency=35 kHz and at 25°C (n=3, mean values).

Time (min)	PHE ₀ ^d	TiO ₂ =2 mg/L ^a ; TiO ₂ =4 mg/L ^b ; TiO ₂ =8 mg/L ^c							
		Control	Initial phenol metabolites concentrations ^d						
			2-PHE ^d	3-PHE ^d	Catechol ^d	4 -methyl catechol ^d	Tyrosol ^d	Quercetin ^d	Caffeic acid ^d
0	2990	2990	4	9	23	15	42	21	30

Time (min)	PHE ₀ ^d	PHER ^e	Phenol degradation metabolites						
			2-PHE ^e	3-PHE ^e	Catechol ^e	4 -methyl catechol ^e	Tyrosol ^e	Quercetin ^e	Caffeic acid ^e
			150 ^a	299	90	64	68	62	63
150 ^b	90	97	84	83	84	84	83	82	85
150 ^c	179	94	72	69	78	77	79	76	75

Time (min)	PHE ₀ ^d	PHER ^e	NiO=4 mg/L ^f ; NiO=7 mg/L ^g ; NiO=10 mg/L ^h						
			Phenol degradation metabolites						
			2-PHE ^e	3-PHE ^e	Catechol ^e	4 -methyl catechol ^e	Tyrosol ^e	Quercetin ^e	Caffeic acid ^e
150 ^f	478	84	61	63	59	60	56	64	61
150 ^g	269	91	81	78	82	81	80	78	82
150 ^h	359	88	69	64	70	73	76	72	71

Time (min)	PHE ₀ ^d	PHER ^e	ZnO=1 mg/L ⁱ ; ZnO=3 mg/L ^k ; ZnO=5 mg/L ^m						
			Phenol degradation metabolites						
			2-PHE ^e	3-PHE ^e	Catechol ^e	4 -methyl catechol ^e	Tyrosol ^e	Quercetin ^e	Caffeic acid ^e
150 ^j	419	86	62	65	60	61	58	65	62
150 ^k	209	93	82	80	83	82	81	80	84
150 ^m	299	90	70	66	72	75	77	74	73

PHE₀: Initial total phenol concentration (mg/L); PHER: Total phenol removal efficiency (%); 2-PHE (%): 2-phenyl-phenol removal efficiency (%); 3-PHE (%): 3-phenyl-phenol removal efficiency (%); ^a TiO₂=2 mg/L.

^b TiO₂=4 mg/L; ^c TiO₂=8 mg/L; ^d Concentration (mg/L); ^e Removal efficiency (%); ^f NiO=4 mg/L; ^g NiO=7 mg/L; ^h NiO=10 mg/L; ⁱ ZnO=1 mg/L; ^k ZnO=3 mg/L; ^m ZnO=5 mg/L.

factors, such as the particle size and surface area, as well the catalyst structure. The maximum conversion of cyclohexane has been observed when nano-sized NiO was used as a catalyst (Srivastava et al., 2003). The utilization of the nano-sized NiO in the treatment of wastewater are limited only with the utilization of this oxide as adsorbent for the removal of dyes from the textile industry wastewaters. Chowdhury et al. (2010) found 78% dye and color yields in a textile industry wastewater using nano-sized NiO as adsorbent. Zhang et al. (2012) found a high adsorption of congo red dye onto nano-sized NiO particles with a color removal of 79%. Similarly, Song et al. (2009) used nano-sized NiO for the removal of dyes from the wastewaters. Microwave-induced degradation of crystal violet dye in the existence of OH group with an atomic percentage of O:Ni: 2.80 to 1 was investigated. This dye was degraded efficiently (73%) under microwave irradiation (2450 MHz) (He et al., 2010).

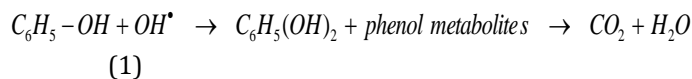
Variation of poly-phenols in the OMW in the presence of nano-sized metal oxides

The treatment by ultrasound converts the poly-phenols in the OMW to much smaller sonodegraded compounds such as tyrosol, hydroxytyrosol, caffeic acid, quercetin, ferulic acid, catechol, vanillic acid, o-quinone, *p*-coumaric acid, *p*-hydroxybenzaldehyde, 4-methyl catechol, 2-PHE and 3-PHE (Wang et al., 2008). Table 6 shows the measured phenol intermediates and their removals in this study (catechol, tyrosol, quercetin, caffeic acid, 4-methyl catechol, 2-PHE and 3-PHE) in the OMW defined with HPLC before ultrasound at t=0 and after 150 min ultrasound times, at pH=5.4 at increasing concentrations of nano-sized metal oxides TiO₂ (2, 4 and 8 mg/L), NiO (4, 7 and 10 mg/L) and ZnO (1, 3 and 5 mg/L) at 25°C.

As shown in Table 6, 2990 mg/L total phenol in the raw wastewater consisted of 23 mg/L catechol, 42 mg/L

tyrosol, 21 mg/L quercetin, 30 mg/L caffeic acid, 15 mg/L 4-methyl catechol, 4 mg/L 2-PHE and 9 mg/L 3-PHE before ultrasound at $t=0$. The phenol metabolite concentrations mentioned above increased to 600, 388, 350, 345, 395, 247 and 268 mg/L with 2 mg/L nano-sized TiO_2 after 120 min ultrasound time, at $\text{pH}=5.40$ and at 30°C (data not shown). Catechol, tyrosol, quercetin, caffeic acid, 4-methyl catechol, 2-PHE and 3-PHE reduced to 280, 220, 190, 185, 195, 123 and 99 mg/L after 150 min ultrasound time, at $\text{pH}=5.4$ and at 30°C (data not shown). These phenol metabolites were removed with yields of 62, 61, 68, 64, 63, 64 and 68%, respectively at a nano-sized TiO_2 concentration of 2 mg/L after 150 min ultrasound time, at $\text{pH}=5.40$ and at 25°C , while 299 mg/L total phenol remained in the sonicator reactor. The catechol, tyrosol, quercetin, caffeic acid, 4-methyl catechol, 2-PHE and 3-PHE removals were 84, 83, 82, 85, 84, 84 and 83%, respectively at nano-sized $\text{TiO}_2=4$ mg/L after 150 min ultrasound time, at 25°C and $\text{pH}=5.40$ with an effluent total phenol concentration of 90 mg/L. The yields of the aforementioned phenol metabolites decreased to 78, 79, 76, 75, 77, 72 and 69%, respectively as the nano-sized TiO_2 concentration was decreased from 4 to 8 mg/L after 150 min ultrasound time, at $\text{pH}=5.40$ and at 25°C (Table 6). Anju et al. (2012) showed that the primary degradation products of phenol were hydroquinone, catechol, and benzoquinone. The differences in the phenol metabolites can be attributed to the differences in wastewater composition, the operational conditions and the nano-sized TiO_2 concentration.

Throughout the simultaneous ultrasound in the presence of nano-sized TiO_2 in the OMW, the bonds in nano-sized TiO_2 could be easily attacked by OH^\bullet and H^+ cations that originate from H_2O_2 and H_2O molecules, respectively, to subsequently form $\text{O}^- \text{Ti}^+ - \text{O}^- \text{OH}^\bullet$ and $\text{O}^- \text{Ti}^+ - \text{OH}^\bullet$ ions. These ions would combine with each other on the surface of original nano-sized TiO_2 particles. The generation of OH^\bullet radicals from the pyrolysis of H_2O during ultrasonic irradiation of phenol is shown in Equation (1):



The phenol metabolite concentrations increased after 60 and 120 min ultrasound time with 4 mg/L nano-sized NiO addition. 550 mg/L catechol, 377 mg/L tyrosol, 330 mg/L quercetin, 314 mg/L caffeic acid, 344 mg/L 4-methyl catechol, 226 mg/L 2-PHE and 251 mg/L 3-PHE were produced with the addition of nano-sized NiO=4 mg/L after 60 min ultrasound time, at $\text{pH}=5.40$ and at 25°C . These phenol metabolites were removed with yields of 59, 56, 64, 61, 60, 61 and 63%, respectively at the aforementioned nano-sized NiO concentration after 150 min ultrasound time, at $\text{pH}=5.40$ and at 25°C , while 478 mg/L total phenol remained in the sonicator reactor. The catechol, tyrosol,

quercetin, caffeic acid, 4-methyl catechol, 2-PHE and 3-PHE removal efficiencies increased to 82, 80, 78, 82, 81, 81 and 78% as the nano-sized NiO concentration was increased from 4 to 7 mg/L after 150 min ultrasound time, at $\text{pH}=5.40$ and at 25°C . The metabolite yields decreased to 70, 76, 72, 71, 73, 69 and 64% at nano-sized NiO=10 mg/L after 150 min ultrasound time, at 30°C and $\text{pH}=5.40$ (Table 6). The increase in degradation yields of phenol metabolites at a 4 mg/L nano-sized NiO concentration can be attributed to the increase in the number of active cavitation bubbles and consequent generation of more OH^\bullet radicals with simultaneous adsorption of metabolites to the aforementioned nano-sized metal oxides.

Catechol, tyrosol, quercetin, caffeic acid, 4-methyl catechol, 2-PHE and 3-PHE were removed with yields of 60, 58, 65, 62, 61, 62 and 65%, respectively in nano-sized ZnO=1 mg/L after 150 min ultrasound time, at $\text{pH}=5.40$ and at 30°C , while 419 mg/L total phenol remained in the sonicator reactor. The removal yields in the phenol metabolites increased to 83, 81, 80, 84, 82, 82 and 80%, respectively in nano-sized ZnO=3 mg/L after 150 min ultrasound time, at 25°C and at $\text{pH}=5.40$. The removal efficiencies decreased to 72, 77, 74, 73, 75, 70 and 66%, respectively as the nano-sized ZnO concentration was increased from 3 to 5 mg/L after 150 min ultrasound time, at $\text{pH}=5.40$ and at 30°C (Table 6). Throughout ultrasound, the highly excited holes on the surface of nano-sized ZnO did not only directly decompose the phenol to their metabolites but also phenol molecules were adsorbed on the surface of nano-sized ZnO nano-particles and oxidize the H_2O to produce OH^\bullet radicals with high activity and indirectly degrade the phenols molecules to their metabolites in the OMW.

It can be assumed that the total phenol concentrations of 90, 269 and 209 mg/L remaining during the ultrasound at nano-sized $\text{TiO}_2=4$ mg/L (see Table 6), nano-sized NiO=7 mg/L and nano-sized ZnO=3 mg/L, respectively at 30°C , after 150 min ultrasound time and at $\text{pH}=5.40$ could not be cleaved to other phenol metabolites, such as hydroxytyrosol, o-quinone, *p*-coumaric acid and *p*-hydroxybenzaldehyde throughout ultrasound since their concentrations were detected as zero. Probably the phenol remaining from the ultrasound can be the phenol which was not converted to corresponding metabolites given above and to the other metabolites not measured in this study (oleuropein, quercetin, ferulic acid and vanillic acid) through ultrasound. In the study by Khoufi et al. (2004), 45% catechol, 52% tyrosol, 42% quercetin, 49% caffeic acid and 30% 2-PHE removal efficiencies were found at a 80 kHz frequency with 140 min ultrasound time. The higher phenol and phenol metabolites removals found in our study could be originated from the composition of the OMW, from the operational conditions such as the ultrasound power, ultrasound intensity, ultrasound frequency and ultrasound

temperature.

Conclusions

The maximum COD_{dis}, color, TAAs and total phenol yields were > 90% with 4 mg/L nano sized-TiO₂, 5 mg/L nano sized-ZnO and 4 mg/L nano sized-TiO₂. The combination of ultrasound and nano-sized metal oxides appears to have a positive synergistic effect on the reduction of COD_{dis}, total phenol, color, TAAs and phenol metabolites from the the OMW. COD_{dis}, phenol by-products and color are mainly eliminated by OH[•] radicals, while the dominant TAAs degradation mechanism is pyrolysis throughout ultrasound.

ACKNOWLEDGEMENT

This research study was conducted in the Environmental Microbiology Laboratory at Dokuz Eylül University Engineering Faculty Environmental Engineering Department, Izmir, Turkey. The authors would like to thank this body for providing financial support.

REFERENCES

- Abu Tarboush BJ, Husein MM, (2012). Adsorption of asphaltenes from heavy oil onto in situ prepared NiO nanoparticles. *J. Colloid. Interface Sci.* 378: 64–69.
- Ahmed MA (2012). Synthesis and structural features of mesoporous NiO/TiO₂ nanocomposites prepared by sol-gel method for photodegradation of methylene blue dye. *J. Photochem. Photobiol: A Chem.* 238: 63–70.
- Anju SG, Yesodharan S, Yesodharan EP (2012). Zinc oxide mediated sonophotocatalytic degradation of phenol in water. *Chem. Eng. J.* 189–190, 84–93.
- Atanassova D, Kefalas P, Petrakis C, Mantzavinis D, Kalogerakis N, Psillakis E (2005). Sonochemical reduction of the antioxidant activity of olive mill wastewater. *Environ. Int.* 31: 281–287.
- Benedito J, Mulet A, Clemente G, Garcia-Perez JV (2004). Use of ultrasonics for the composition assessment of olive mill wastewater (alpechin). *Food Res. Int.* 37: 595–601.
- Bertin L, Majone M, Di Gioia D, Fava F (2001). An aerobic fixed-phase biofilm reactor system for the degradation of the low-molecular weight aromatic compounds occurring in the effluents of anaerobic digestors treating olive mill wastewaters. *J. Biotechnol.* 87: 161–177.
- Canizares-Macias MP, Garcia-Mesa JA, Lague de Castro MD (2004). Fast ultrasound-assisted method for the determination of the oxidative stability of virgin olive oil. *Analyt. Chim. Acta* 502: 161–166.
- Cardoso SM, Mafra I, Reis A, Nunes C, Saraiva JA, Coimbra MA (2010). Naturally fermented black olives: effect on cell wall polysaccharides and on enzyme activities of Taggiasca and Conservolea varieties. *LWT-Food Sci. and Technol.* 43: 153–160.
- Chowdhury AN, Rahim A, Ferdosi YJ, Azam Md.S, Hossain MM (2010). Cobalt-nickel mixed oxide surface: A promising adsorbent for the removal of PR dye from water. *Appl. Surf. Sci.* 256: 3718–3724.
- Currell DL, Wilhelm G, Nagy S (1963). The effect of certain variables on the ultrasonic cleavage of phenol and of pyridine. *J. Am. Chem. Soc.* 85: 127–130.
- David B (2009). Sonochemical degradation of PAH in aqueous solution. Part I: Monocomponent PAH solution. *Ultrason. Sonochem.* 16: 260–265.
- Drijvers D, Langenhove HV, Beckers M (1999). Decomposition of phenol and trichloroethylene by the ultrasound/H₂O₂/CuO process. *Water Res.* 33: 1187–1194.
- Eaton AD, Clesceri LS, Rice EW, Greenberg AE, Franson MAH (2005). Standard Methods for the Examination of Water and Wastewater, in: Franson, M.A.H. (Eds.), twenty first ed. American Public Health Association (APHA), American Water Works Association (AWWA), Water Environment Federation (WEF). American Public Health Association 800 I Street, NW Washington DC: 20001-3770, USA.
- El Hajjoui H, Merlina G, Pinelli E, Winterton P, Revel JC, Hafidi M (2008). ¹³C NMR study of the effect of aerobic treatment of olive mill wastewater (OMW) on its lipid-free content. *J. Hazard. Mater.* 154: 927–932.
- Francioso O, Ferrari E, Saladini M, Montecchio D, Gioacchini P, Ciavatta C (2007). TG-DTA, DRIFT and NMR characterisation of humic-like fractions from olive wastes and amended soil. *J. Hazard. Mater.* 149: 408–417.
- He H, Yang S, Yu K, Ju Y, Sun C, Wang L (2010). Microwave induced catalytic degradation of crystal violet in nano-nickel dioxide suspensions. *J. Hazard. Mater.* 173: 393–400.
- Khokhawala IM, Gogate PR, (2010). Degradation of phenol using a combination of ultrasonic and UV irradiations at pilot scale operation. *Ultrason. Sonochem.* 17: 833–888.
- Khoufi S, Aouissou H, Penninckx M, Sayadi S (2004). Application of electro-fenton oxidation for the detoxification of olive mill wastewater phenolic compounds. *Water Sci. Technol.* 49: 97–102.
- Lafi WK, Shannak B, Al-Shannag M, Al-Anber Z, Al-Hasan M (2009). Treatment of olive mill wastewater by combined advanced oxidation and biodegradation. *Sep. Purif. Technol.* 70: 141–146.
- Laxmi PNV, Sarithaa P, Rambabua N, Himabindua V, Anjaneyulu Y (2010). Sonochemical degradation of 2-chloro-5-methyl phenol assisted by TiO₂ and H₂O₂. *J. Hazard. Mater.* 174: 151–155.
- Olthof M, Eckenfelder WW Jr., (1976). Coagulation of textile wastewater. *Text. Chem. Color.* 8: 18–22.
- Pang YL, Abdullah AZ, Bhatia S (2011). Review on sonochemical methods in the presence of catalysts and chemical additives for treatment of organic pollutants in wastewater. *Desalination.* 277: 1–14.
- Petrier C, Lamy MF, Francony A, Benahcene A, David B, Renaudin V, Gondrexon NJ (1994). Sonochemical degradation of phenol in dilute aqueous solutions: Comparison of the reaction rates at 20 and 487 kHz. *J. Phys. Chem.-US* 98: 10514–10520.
- Silva AMT, Nouli E, Carmo-Apolinário AC, Xekoukoulotakis NP, Mantzavinis D (2007). Sonophotocatalytic/H₂O₂ degradation of phenolic compounds in agro-industrial effluents. *Catal. Today.* 124: 232–239.
- Song Z, Chen LF, Hu JC, Richards R (2009). NiO(111) nanosheets as efficient and recyclable adsorbents for dye pollutant removal from wastewater. *Nanotechnology* 20, art. No 275707. pp.9.
- Sponza DT, Oztekin R (2011). Contribution of oxides, salt, and carbonate to the sonication of some hydrophobic polyaromatic hydrocarbons and toxicity in petrochemical industry wastewater in Izmir, Turkey. *J. Environ. Eng.-ASCE* 137: 1012–1025.
- Srivastava DN, Perkas N, Seisenbaeva GA, Kolytyn Y, Kessler VG, Gedanken A (2003). Preparation of porous cobalt and nickel oxides from corresponding alkoxides using a sonochemical technique and its application as a catalyst in the oxidation of hydrocarbons. *Ultrason. Sonochem.* 10: 1–9.
- Uğurlu M, Karaoğlu MH (2011). TiO₂ supported on sepiolite: Preparation, structural and thermal characterization and catalytic behaviour in photocatalytic treatment of phenol and lignin from olive mill wastewater. *Chem. Eng. J.* 166: 859–867.
- Villeneuve L, Alberti L, Steghens JP, Lancelin JM, Mestas JL (2009). Assay of hydroxyl radicals generated by focused ultrasound. *Ultrason. Sonochem.* 16: 339–344.
- Wang J, Jiang Z, Zhang Z, Xie Y, Wang X, Xing Z, Xu R, Zhang X (2008).

Sonocatalytic degradation of acid red B and rhodamine B catalyzed by nano-sized ZnO powder under ultrasonic irradiation. *Ultrason. Sonochem.* 15: 768-774.

Wu CH (2008). Effects of sonication on decolorization of C.I. reactive red 198 in UV/ZnO system. *J. Hazard. Mater.* 153: 1254-1261.

Wu Z, Ondruschka B (2005). Roles hydrophobicity and volatility of organic substrates on sonolytic kinetics in aqueous solutions. *J. Phys. Chem.-US* 109: 6521-6526.

Zhang P, Ma X, Guo Y, Cheng Q, Yang L (2012). Size-controlled synthesis of hierarchical NiO hollow microspheres and the adsorption for congo red in water. *Chem. Eng. J.* 189-190: 188-195.

Cite this article as:

Sponza DT, Oztekin R (2019). Degradation of the olive mill industry wastewater with sonication: Effects of some nano metal oxides on sonication. *Acad. J. Sci. Res.* 7(7): 389-402.

Submit your manuscript at

<http://www.academiapublishing.org/ajsr>